

Integrated Front-End Electronics for SiPM Detectors in Medical Imaging Applications

F. Corsi, M. Foresta, F. Licciulli, C. Marzocca, G. Matarrese

DEE - Politecnico di Bari and INFN - Sezione di Bari, Italy



Outline

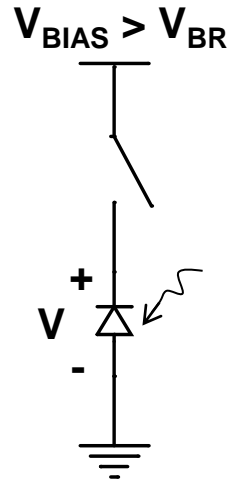
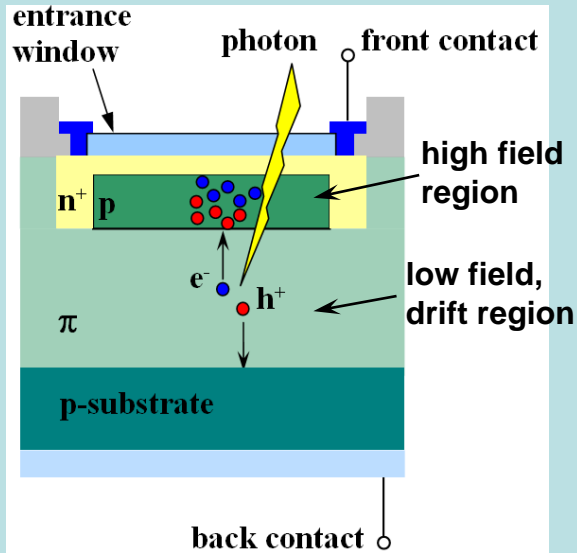
- ❑ Silicon Photo-Multipliers: a short introduction
- ❑ SiPM model and characterization
- ❑ Front-end architecture: different approaches
- ❑ Structure and design of the analog channel
- ❑ Architecture and design of multichannel ASICs: some examples and results
- ❑ Alternative architecture
- ❑ Temperature compensation of SiPM gain
- ❑ Future work



SPAD

Single Photon Avalanche Diode, working in Geiger mode

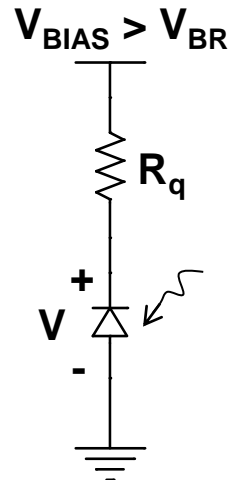
The photodiode is reverse biased above the breakdown voltage V_{BR}



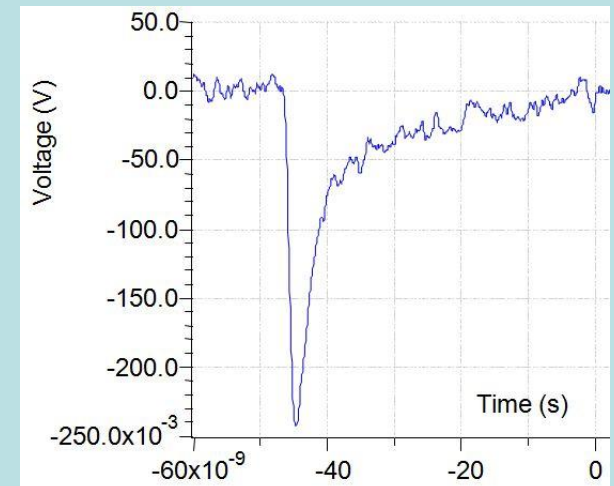
- ❑ Avalanche breakdown triggered by an absorbed photon
- ❑ No charge is extracted: the voltage across the device decreases very quickly and the avalanche is quenched when $V = V_{BR}$
- ❑ The device is recharged to the bias voltage V_{BIAS} and is ready to detect another photon
- ❑ Total charge generated: $Q = C_{\text{pixel}} (V_{BIAS} - V_{BR})$
 $V_{BIAS} - V_{BR} = \Delta V = \text{overvoltage}$

Passive quenching

- ❑ A large resistor R_q is used to quench the avalanche
- ❑ After an avalanche, the device is recharged with a recovery time constant $\tau_R = R_q C_{\text{pixel}}$

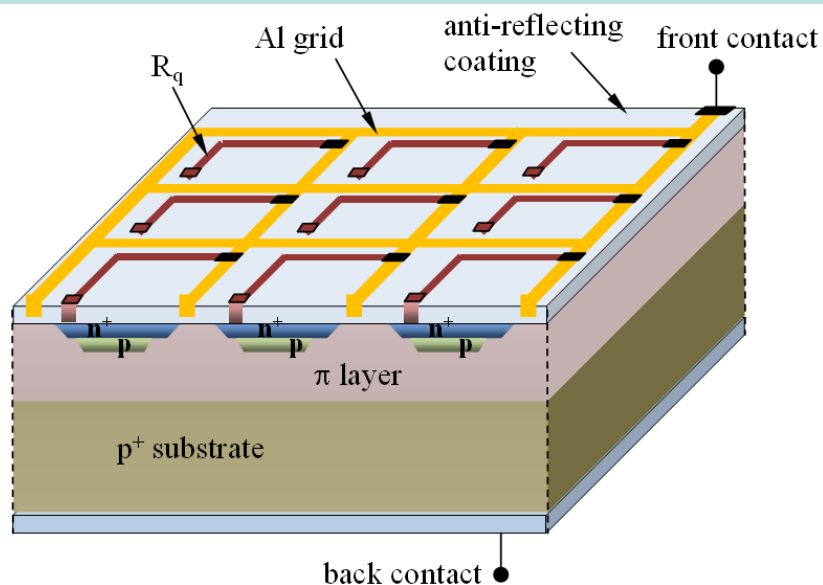


Typical pulse waveform



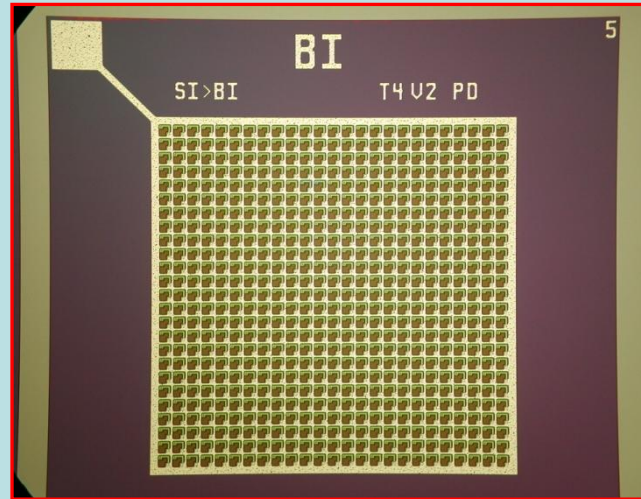
From SPAD to SiPM

Silicon Photo-Multiplier: array of N passively quenched SPAD connected in parallel



Main features

- ❑ Total charge proportional to the no. of incident photons
- ❑ Photon Detection Efficiency = $\epsilon_{\text{GEOM}} \times \text{QE} \times \epsilon_{\text{AVALANCHE}}$
- ❑ High gain $\cong 10^6$
- ❑ Good timing accuracy
- ❑ Low bias voltage
- ❑ Compact and rugged
- ❑ Insensitive to magnetic fields
- ❑ Low cost



SiPM from FBK-irst

Size: 1mm x 1mm

N=25x25

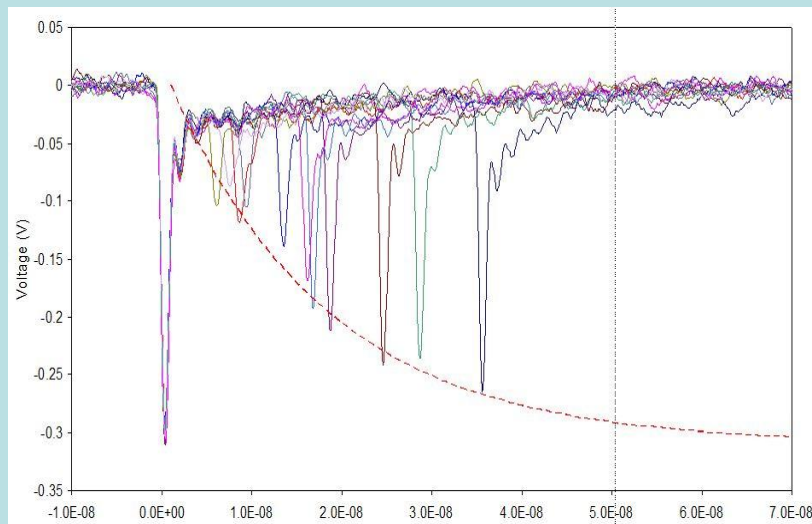
Micro-cell size= 40 μ m x 40 μ m

Applications

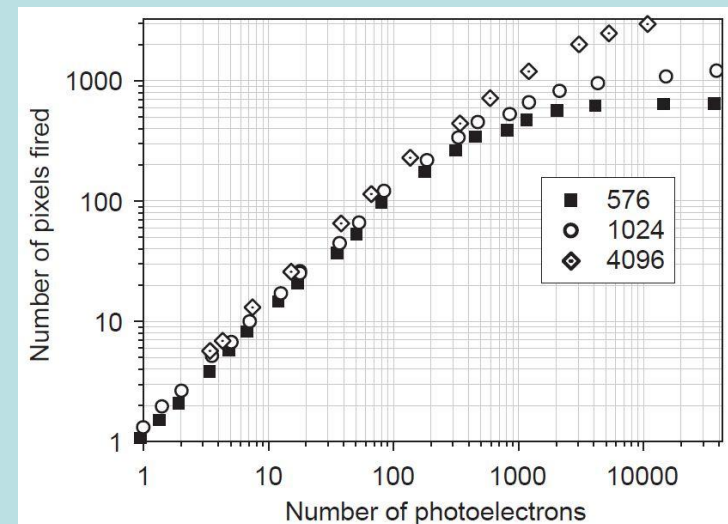
- ❑ Medical imaging (PET, SPECT, ...)
- ❑ HEP (calorimeters, scintillating fibers, ...)
- ❑ Astroparticle physics experiments
- ❑ Detection of low level of light (laser-range finding, photon counting, ...)

SiPM: main limitations

- ❑ Dark count : an avalanche can be triggered by thermally generated electrons
- ❑ Optical cross-talk: a photon can be emitted by a micro-cell undergoing avalanche breakdown and can trigger another avalanche in an adjacent micro-cell
- ❑ Afterpulsing: the avalanche can be retriggered in a micro-cell during the recovery phase, due to the release of carriers trapped in deep energy levels
- ❑ Gain drift with the temperature
- ❑ Saturation: the probability that one micro-cell is hit by more than one photon becomes significant



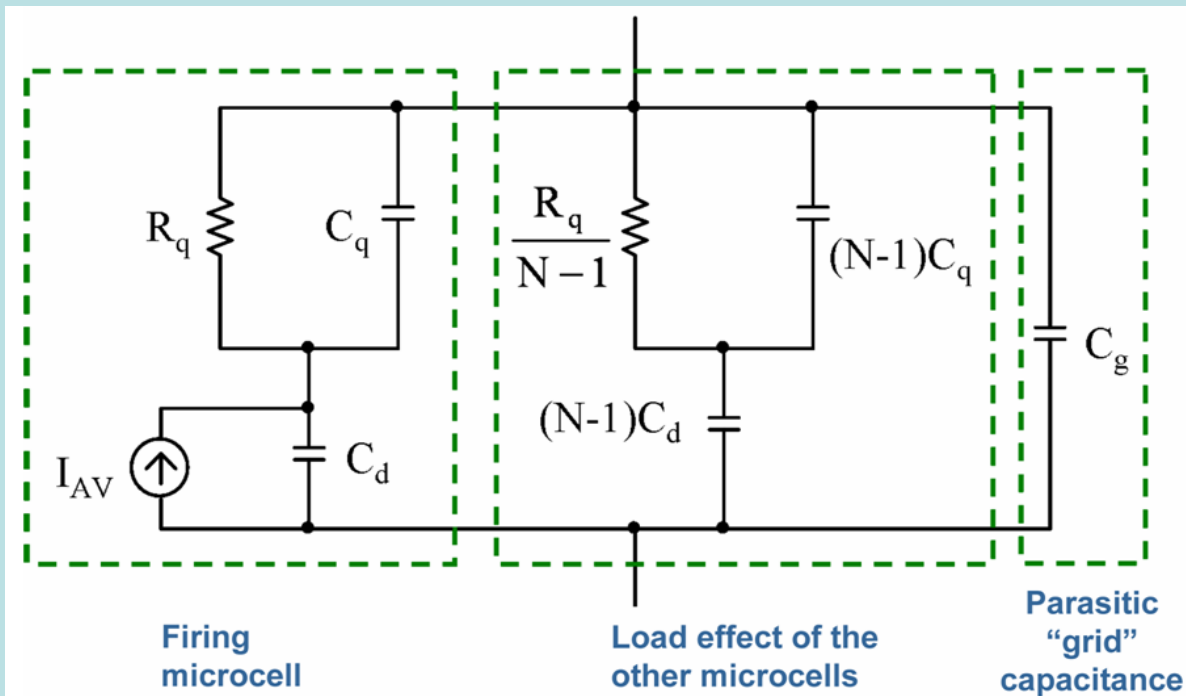
Afterpulsing



Saturation

(V. Andreev et al., NIMA 540, pp. 368-380 (2005))

SiPM model



R_q : quenching resistor
(hundreds of $k\Omega$)

C_d : photodiode capacitance
(few tens of fF)

C_q : parasitic capacitance
(smaller than C_d)

I_{AV} : short current pulse
containing the charge Q
delivered by a single
micro-cell during the avalanche

□ C_g : parasitic capacitance due to the routing of the bias voltage to the N microcells, realized with a metal grid.

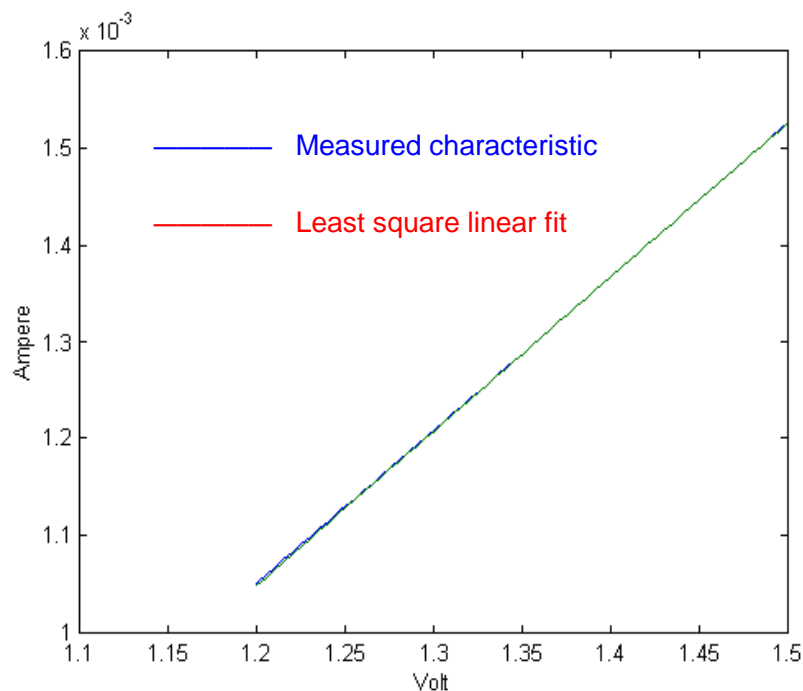
Example: metal-substrate unit area capacitance 0.03 fF/mm^2
metal grid = 35% of the total detector area = 1 mm^2



$C_g \cong 10 \text{ pF}$, without considering the fringe parasitics

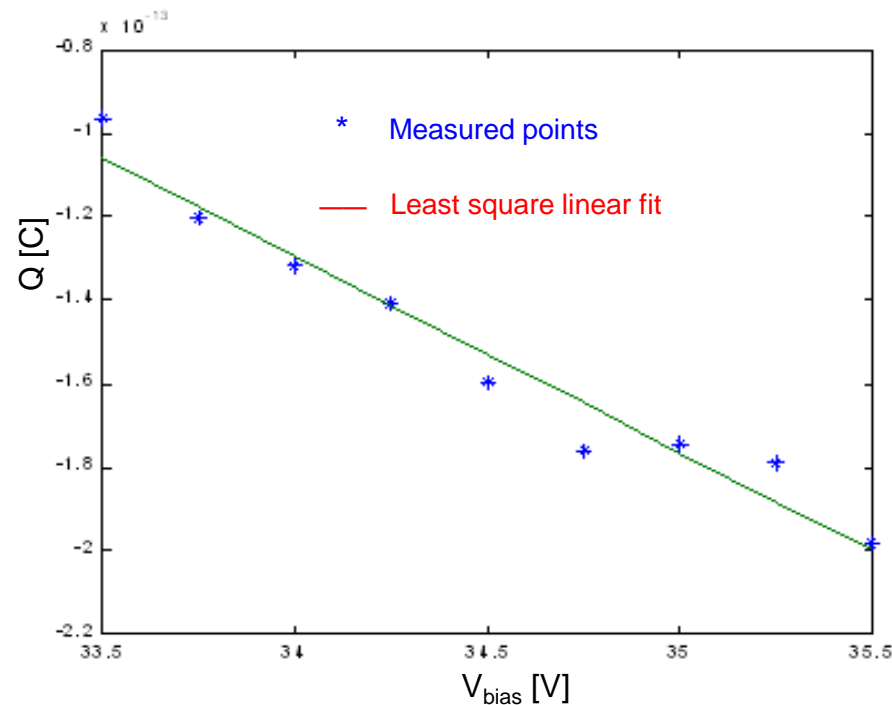
Parameter extraction I

R_q : forward characteristic of the SiPM
(slope almost constant and equal to R_q/N)



*Forward characteristic of a SiPM
manufactured by FBK-Irst.*

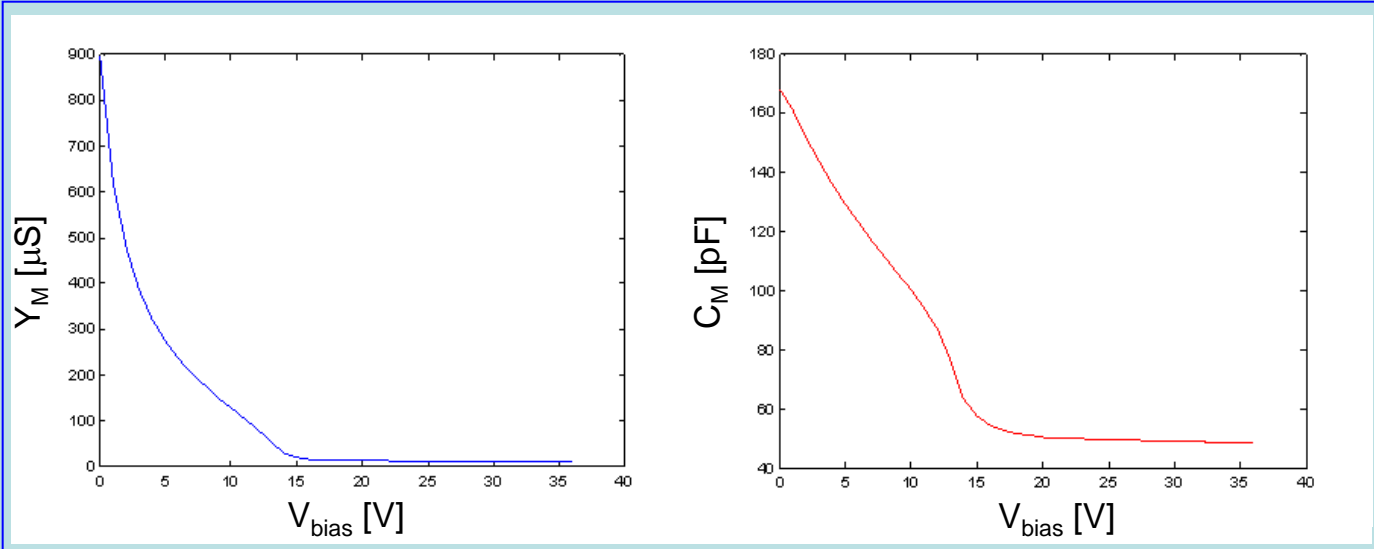
(C_d+C_q) and V_{BR} : charge associated to a single
dark pulse as a function of the bias voltage
 $Q=(C_d+C_q)(V_{BIAS}-V_{BR})$



*Charge contained in a single dark
count pulse vs. bias voltage*

Parameter extraction II

- CV plotter measurements of the SiPM near the breakdown voltage: Y_M and C_M
- According to the SiPM model, Y_M and C_M are expressed in terms of $C_{dtot}=NC_d$, $C_{qtot}=NC_q$, $R_{qtot}=R_q/N$ and the frequency ω of the signal used by the CV plotter.

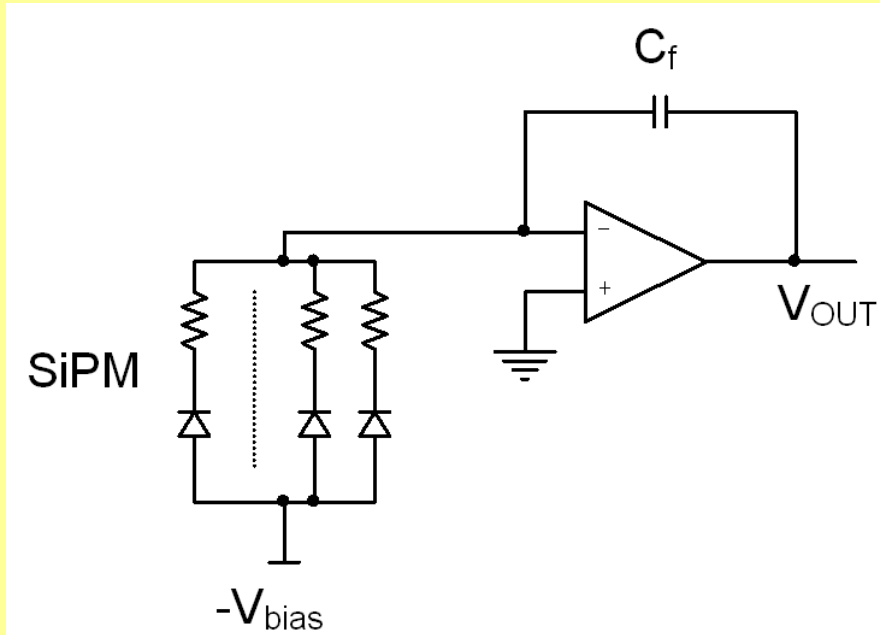


CV plotter measurement results for a SiPM manufactured from FBK-Irst.

$$Y_M = \frac{\omega^2 R_{qtot} C_{dtot}^2}{1 + \omega^2 R_{qtot}^2 C_t^2} \cong \omega^2 R_{qtot} C_{dtot}^2 \quad (C_t = C_{dtot} + C_{qtot}) \longrightarrow C_d, C_q$$

$$C_M = \frac{C_{dtot} + C_g + \omega^2 R_{qtot}^2 C_t (C_g C_t + C_{qtot} C_{dtot})}{1 + \omega^2 R_{qtot}^2 C_t^2} \cong C_{dtot} + C_g \longrightarrow C_g$$

Front-end electronics: different approaches I



Charge Sensitive Amplifier

The charge delivered by the detector is collected on C_f

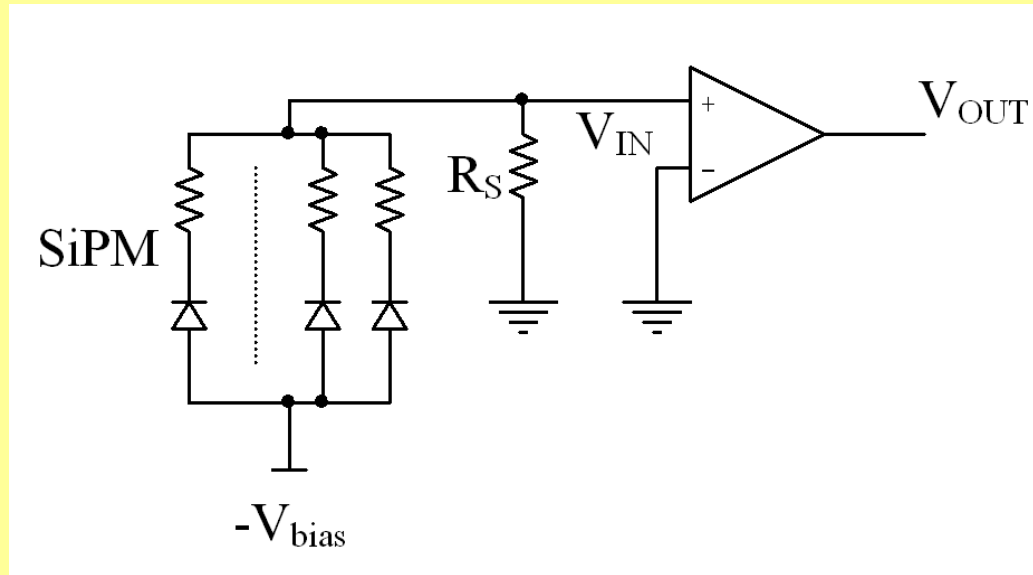
Example:

Maximum ΔV_{OUT} :	3V
SiPM gain:	10^6
No of hit microcells:	300
Total charge Q_{TOT} :	48pC

Large integration capacitance needed: $C_f = 16pF$

- ❑ Dynamic range problems
- ❑ Large silicon area required
- ❑ Large capacitive loads: power consumption issues or bandwidth limitations

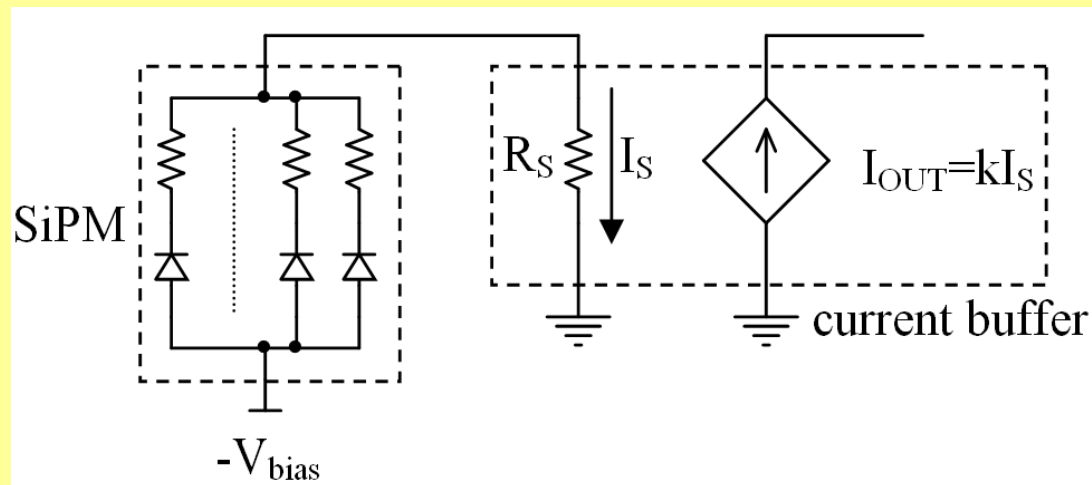
Front-end electronics: different approaches II



Voltage Amplifier

- ❑ A current-to-voltage conversion of the SiPM signal is realized by means of R_S
- ❑ Often used for characterization purposes
- ❑ V_{OUT} must be integrated to extract the charge information: further V-I conversion needed
- ❑ No virtual ground at the amplifier input: R_S must be small to preserve linearity
- ❑ Small R_S : large gain, wide-bandwidth voltage amplifier required (power consumption issues)

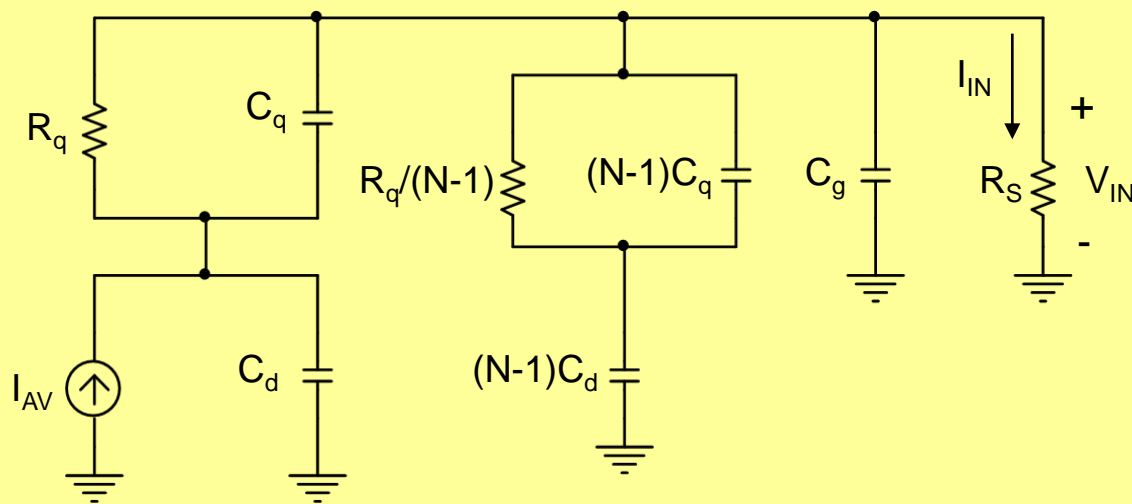
Front-end electronics: different approaches III



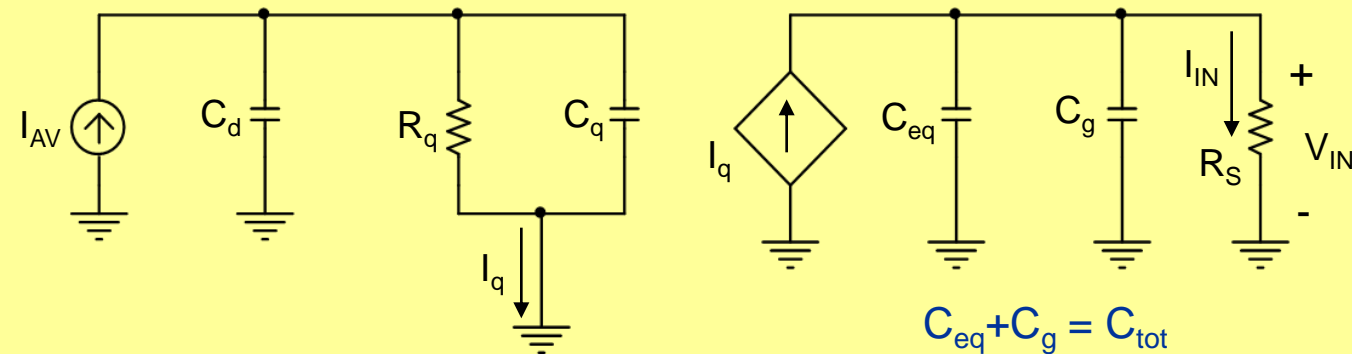
Current Amplifier

- ❑ R_S is the very small input impedance of the current amplifier
- ❑ The output current can be easily replicated (e.g. by means of current mirrors) and further processed (e.g. integrated)
- ❑ The circuit is inherently fast (low impedance nodes)
- ❑ Less problems of dynamic range, also for decreasing supply voltages

SiPM coupled to the front-end



A) SiPM coupled to an amplifier with input impedance R_S

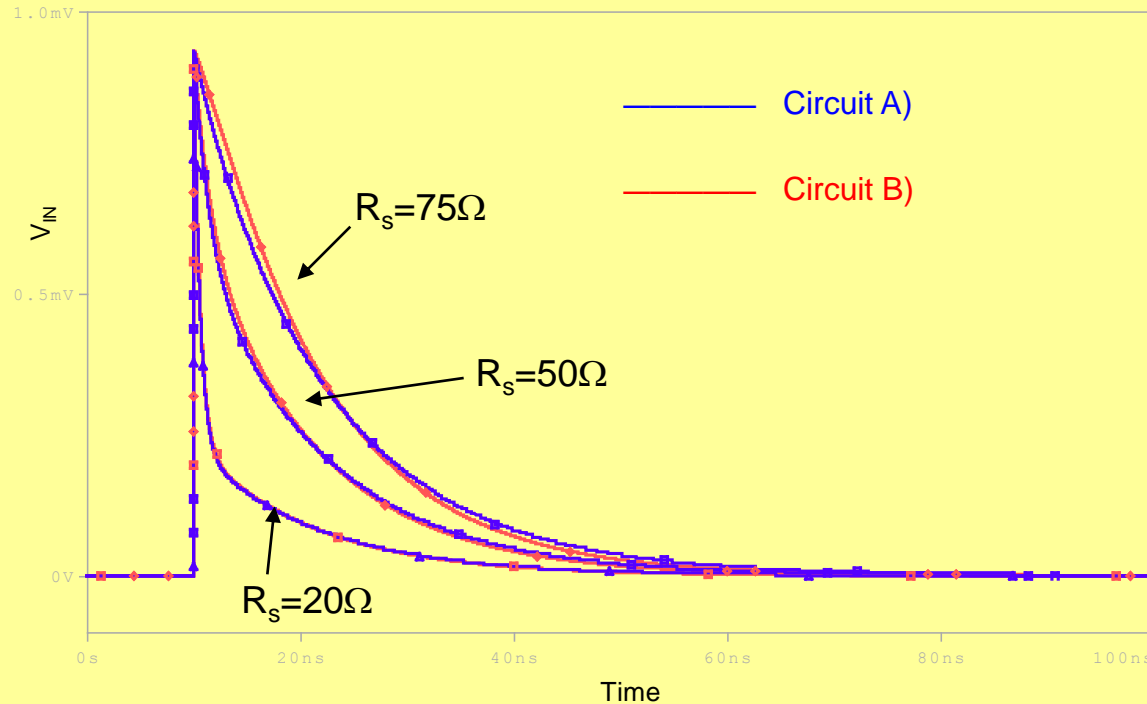


$$\frac{1}{C_{eq}} = \frac{1}{(N-1)C_d} + \frac{1}{(N-1)C_q}$$

$$C_{eq} + C_g = C_{tot}$$

B) Simplified circuit ($R_S \ll R_q/N$)

SiPM + front-end behaviour



Response of the circuits A) and B) to a single dark pulse (160fC) for three different values of R_s and typical parameter values

$$V_{IN}(t) \cong \frac{QR_s}{\tau_r - \tau_{IN}} \left(\frac{\tau_q - \tau_{IN}}{\tau_{IN}} \exp\left(-\frac{t}{\tau_{IN}}\right) + \frac{\tau_r - \tau_q}{\tau_r} \exp\left(-\frac{t}{\tau_r}\right) \right)$$

$$(\tau_q = R_q C_q)$$

Simplified circuit: two time constants

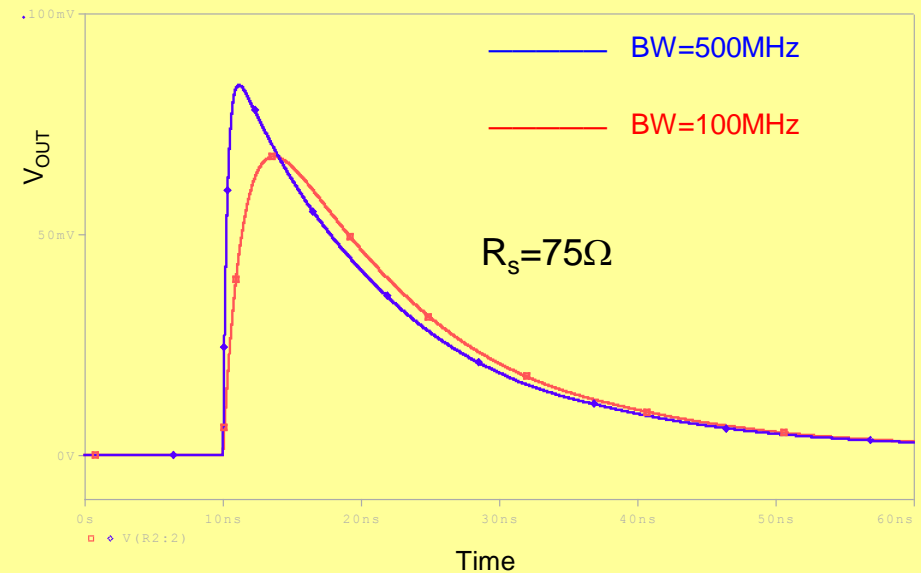
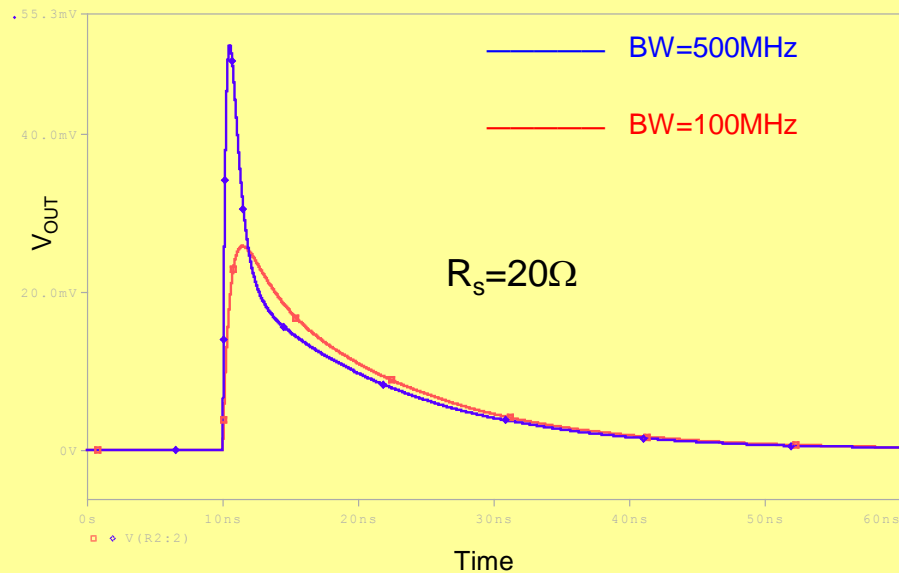
- $\tau_{IN} = R_s (C_{eq} + C_g) = R_s C_{tot}$
- $\tau_r = R_q (C_d + C_q)$

The peak of V_{IN} is almost independent of R_s

A fraction Q_{IN} of the charge Q delivered during the avalanche is almost instantly collected on C_{tot}

$$V_{INMAX} \cong \frac{Q_{IN}}{C_{tot}} \quad Q_{IN} = Q \frac{C_q}{C_d + C_q}$$

Bandwidth of the amplifier

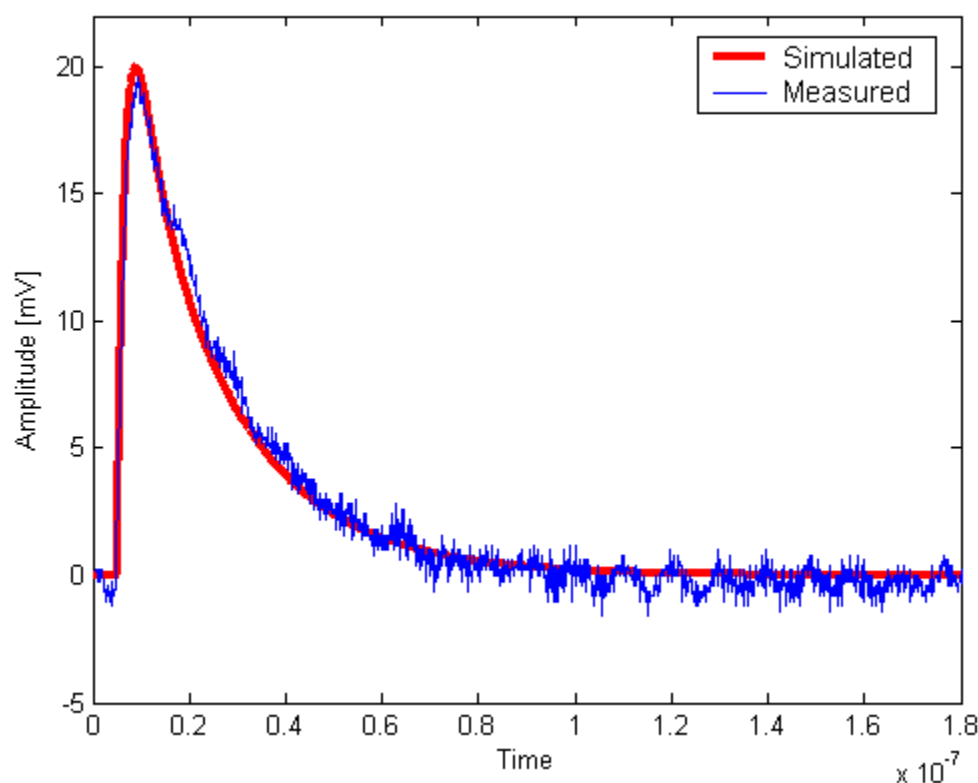


Amplifier output voltage for a single dark pulse: same gain and different bandwidth

- The bandwidth of the amplifier directly affects the **rise time** of the waveform
- The **peak** of the waveform is strongly dependent on the amplifier bandwidth, especially for low values of R_s
- The **time needed to collect the charge** is also slightly influenced by the amplifier bandwidth
- The same conclusions are valid also for the waveform of the output current obtained with a current amplifier

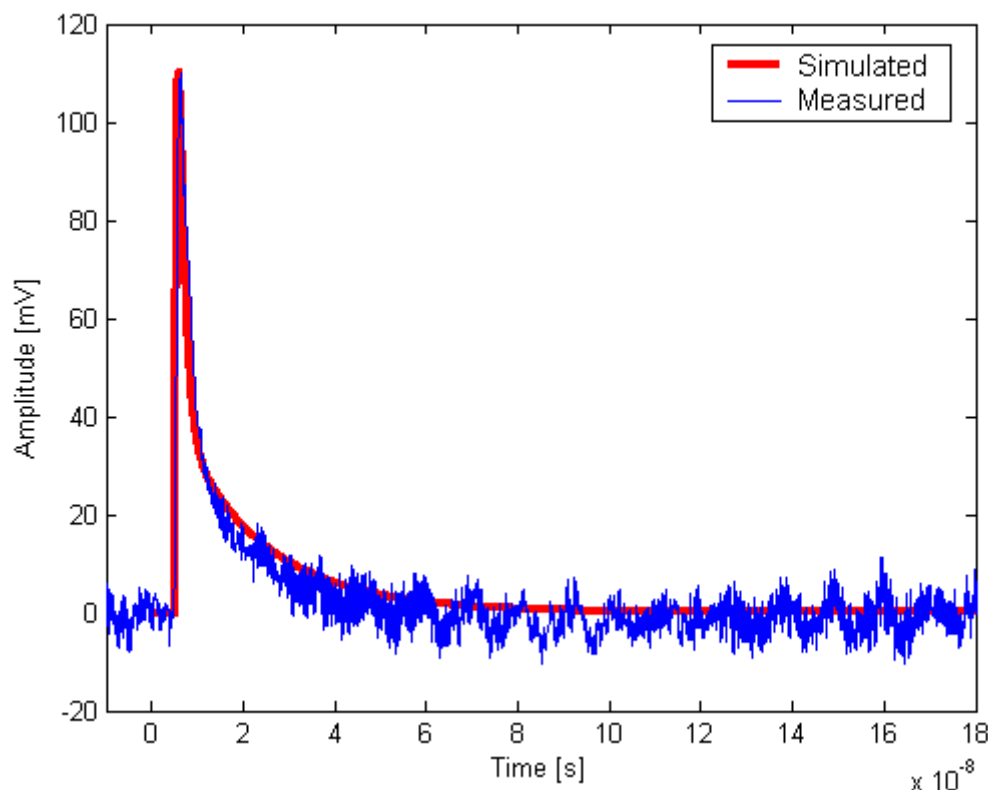
Model validation

Two different amplifiers have been used to read-out the same SiPM (FBK-Irst N = 625, micro-cell size $40 \times 40 \mu\text{m}^2$)



a) Transimpedance amplifier (discrete BJTs)

BW=80MHz $R_s=110\Omega$ Gain=2.7k Ω

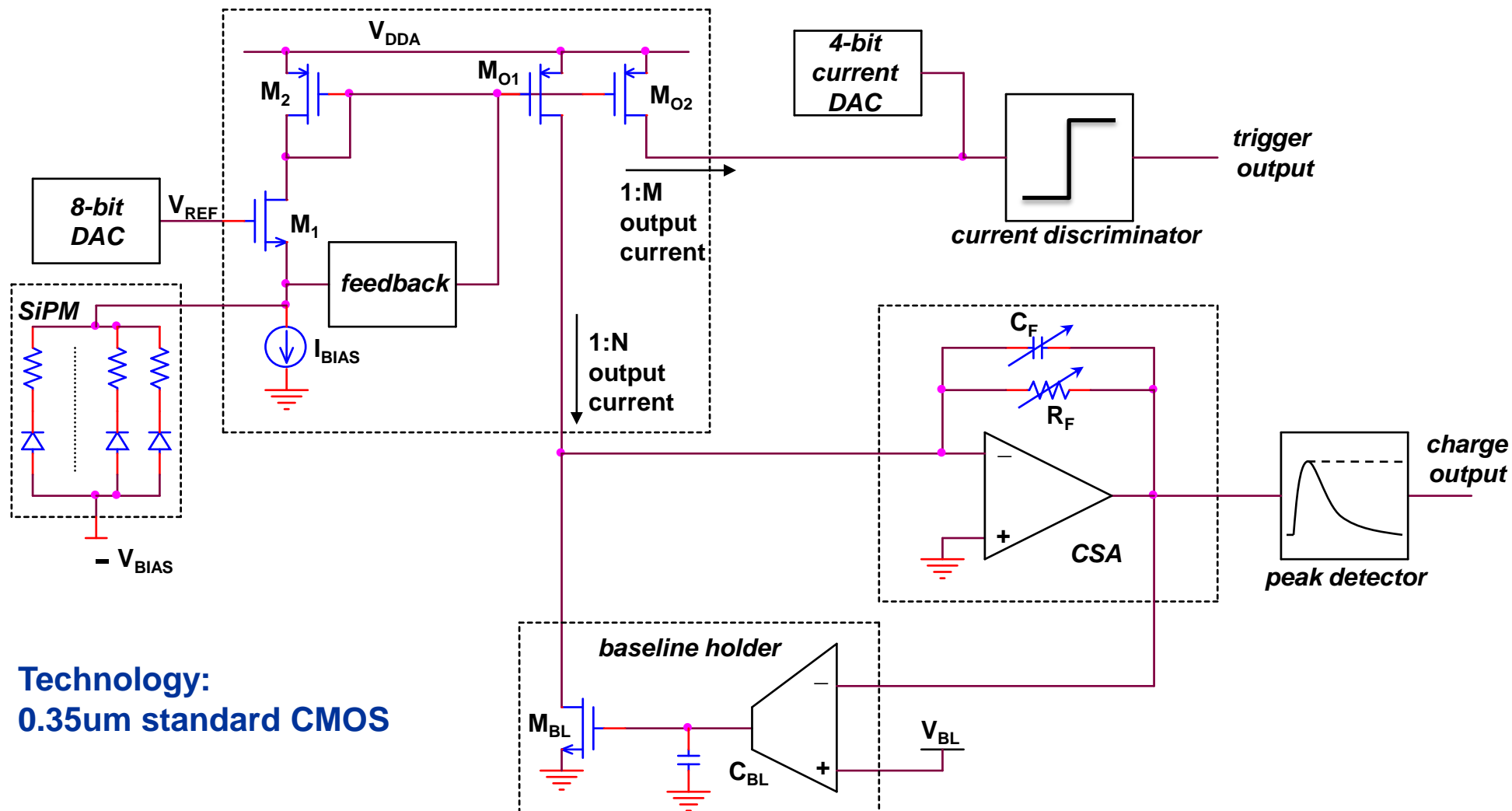


b) Voltage amplifier (hybrid RF circuit)

BW=360MHz $R_s=50\Omega$ Gain=140

- The model extracted according to the procedure described above has been used in the SPICE simulations
- The fitting between simulations and measurements is quite good

Structure of the analog channel



Main features and parameters of the analog channel

Current buffer

- ❑ Small signal bandwidth: 250MHz (with a 30pF detector)
- ❑ Low input resistance: 17Ω
- ❑ Scaling factors: $N=10$, $M=20$
- ❑ V_{REF} variable in the range $1V \div 2V$
- ❑ Total current consumption: $800\mu A$

Fast Current Discriminator

- ❑ Leading edge
- ❑ $T_{rise} \approx 300ps$
- ❑ Threshold programmable :
4-bit current DAC from 0 to $40\mu A$

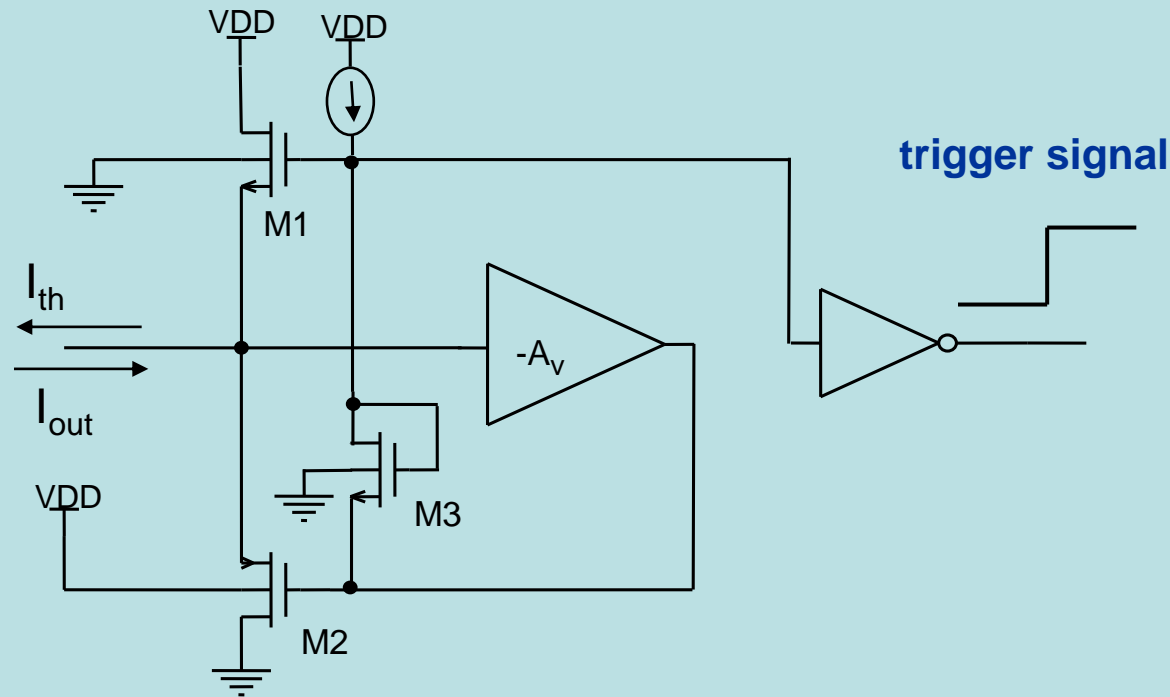
CSA

- ❑ Continuous passive reset
- ❑ Variable gain: $C_F=1pF$, $2pF$, $3pF$
- ❑ Damping time constant: 200ns
- ❑ Output voltage range: $0.3V \div 2.7V$

Baseline holder

- ❑ Very slow feedback loop
- ❑ “Ad hoc” techniques to reproduce large time constants
- ❑ Small baseline shifts at high event rates ($-1mV$ @ 100kHz, full dynamic range)

The current discriminator

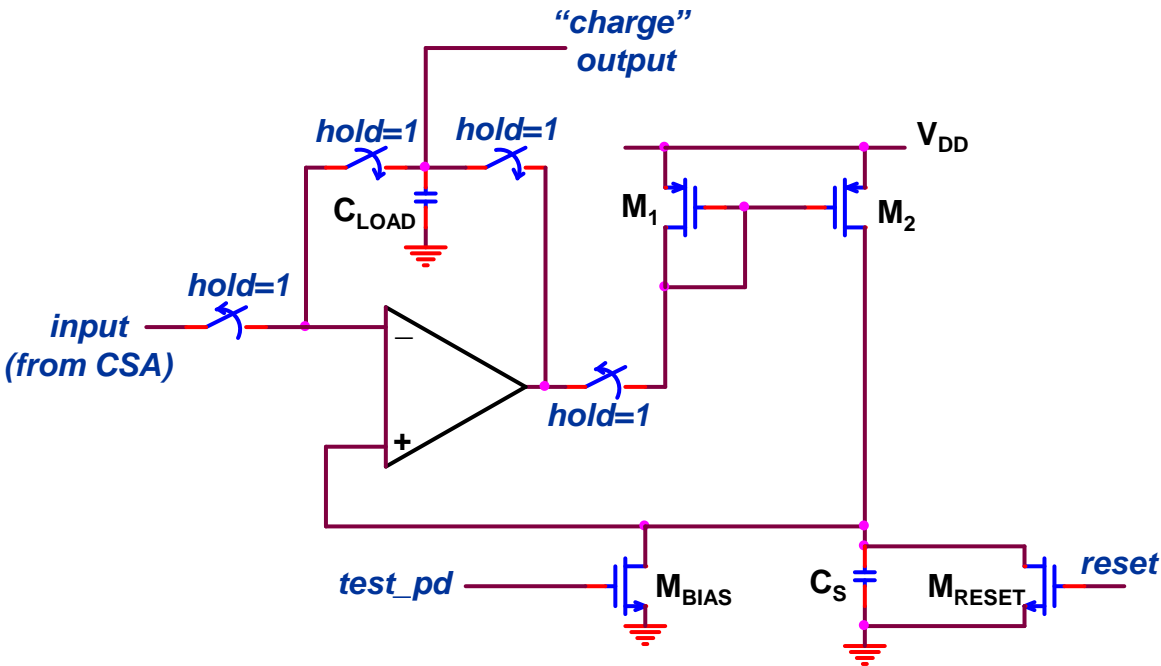


Principle of operation

If I_{out} is less than I_{th} , then M_1 is on and M_2 is off. When I_{out} becomes greater than I_{ref} , the MOSFETs switch and the amplifier output goes low, thus the inverter output goes high

Peak detector modes of operation

- Logic control signals involved: “hold” and “test_pd”



test_pd=1, hold=0: voltage follower

The voltage on C_S follows the CSA output , thanks to the current of M_{BIAS}

test_pd=0, hold=0: peak detector

The voltage on C_S tracks the peak of the CSA output (M_{BIAS} is OFF)

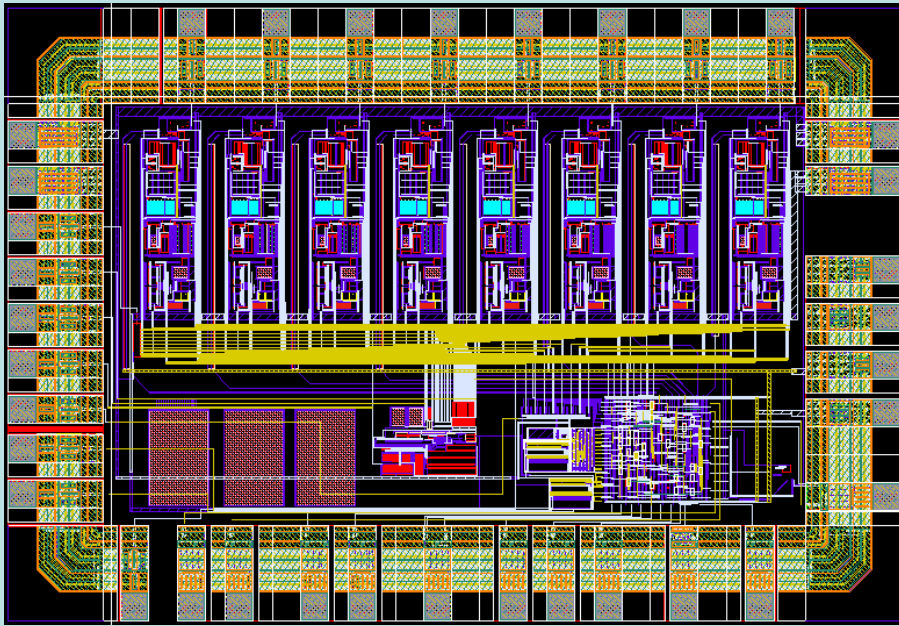
test_pd=0, hold=1: buffer

The voltage stored on C_S is buffered and transferred to the output of the circuit.

Multichannel ASICs available

BASIC8

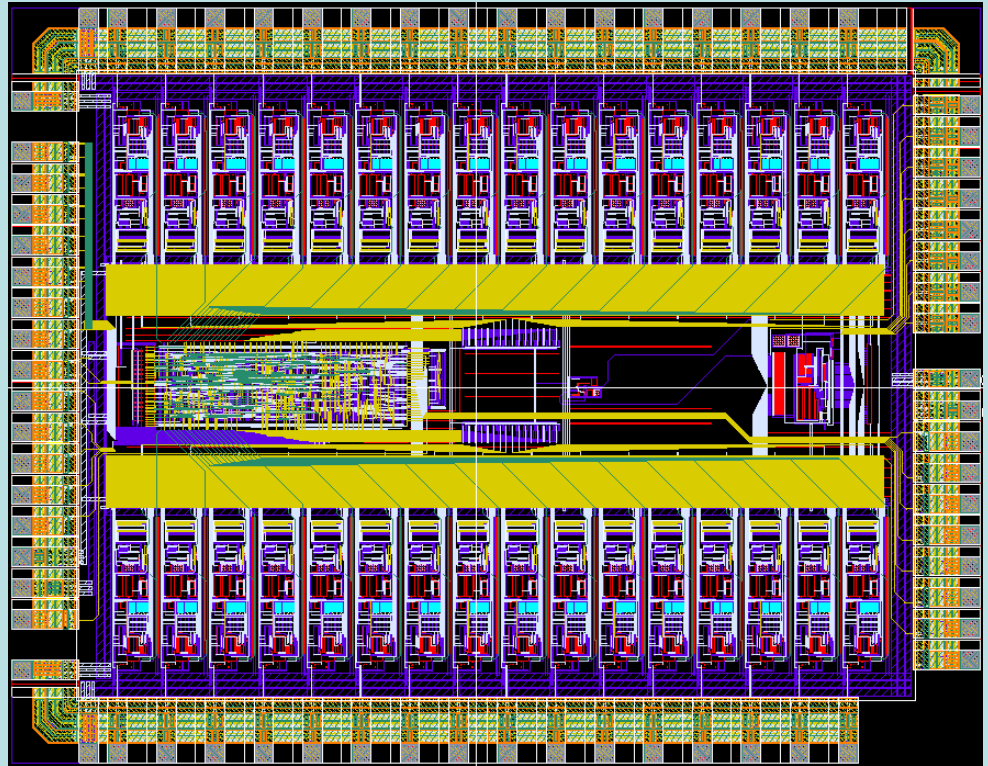
- ❑ 8 channels
- ❑ “Sparse” and “serial” read-out modes
- ❑ 8 bit SAR integrated ADC



Layout of BASIC8 (3.2 x 2.2 mm²)

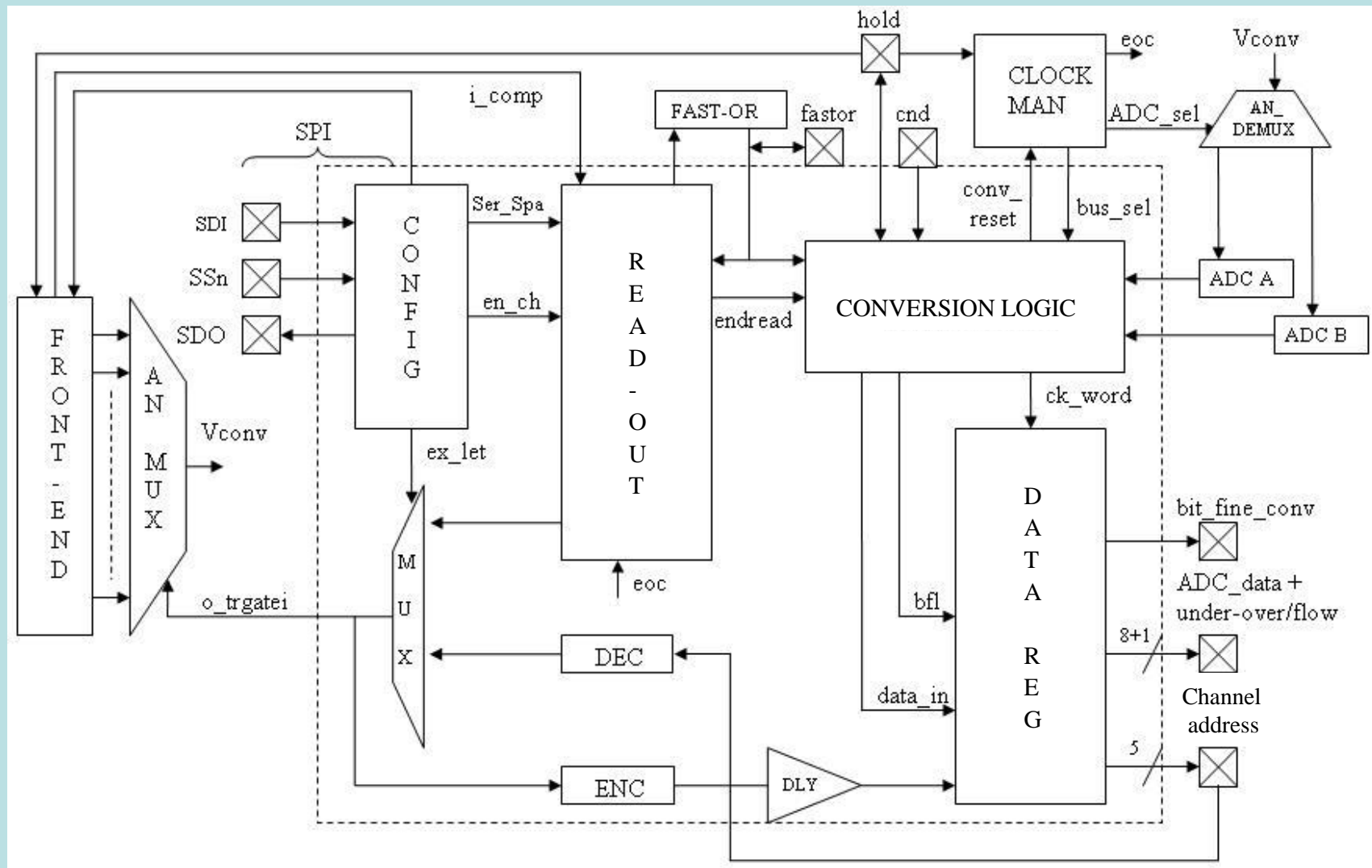
BASIC32

- ❑ 32 channels
- ❑ Enhanced programmability and RO modes
- ❑ No integrated ADC



Layout of BASIC32 (5 x 3.9 mm²)

BASIC32: block diagram



BASIC32: main features

Acquisition modes

Internal read-out

Internal trigger (“fast-OR”) } Sparse
External trigger } Serial

External read-out

External control of the PD’s
External channel addressing



Multiplexing, PD control and reset of the channels managed by the read-out logic

Configuration logic

- ☐ SPI interface
- ☐ 56-bit configuration word
- ☐ Verification features

Read-out logic

- ☐ Multiplexer management
- ☐ Fast-or management
- ☐ Masking and reset of the channels

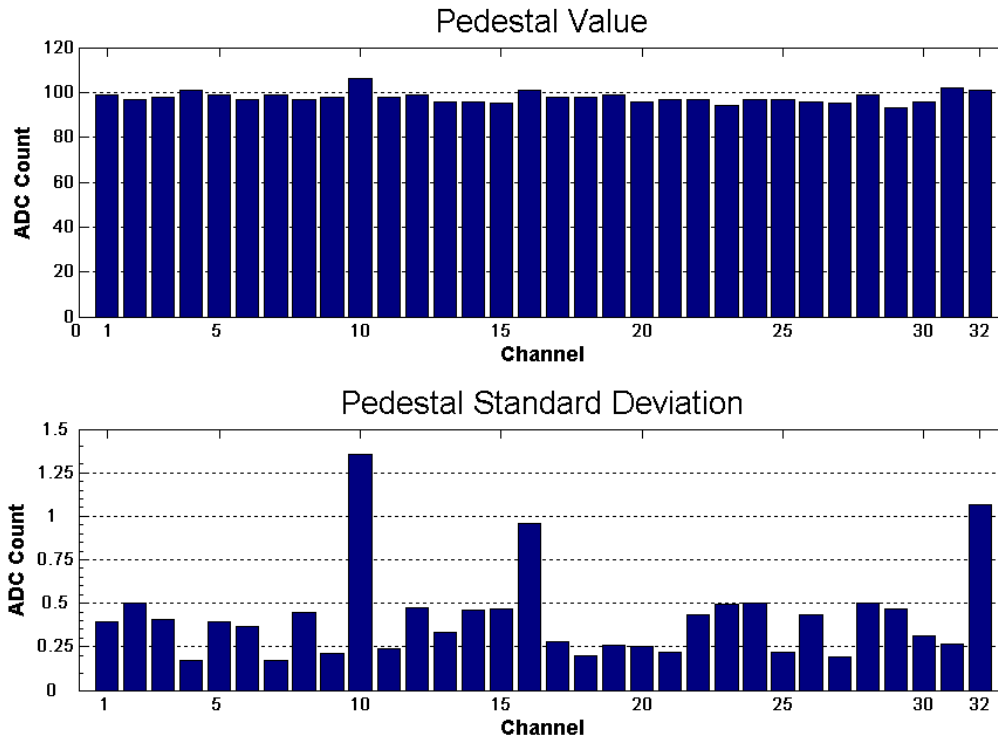
Conversion logic

- ☐ ADC management
- ☐ Data flow management

Coincidence management

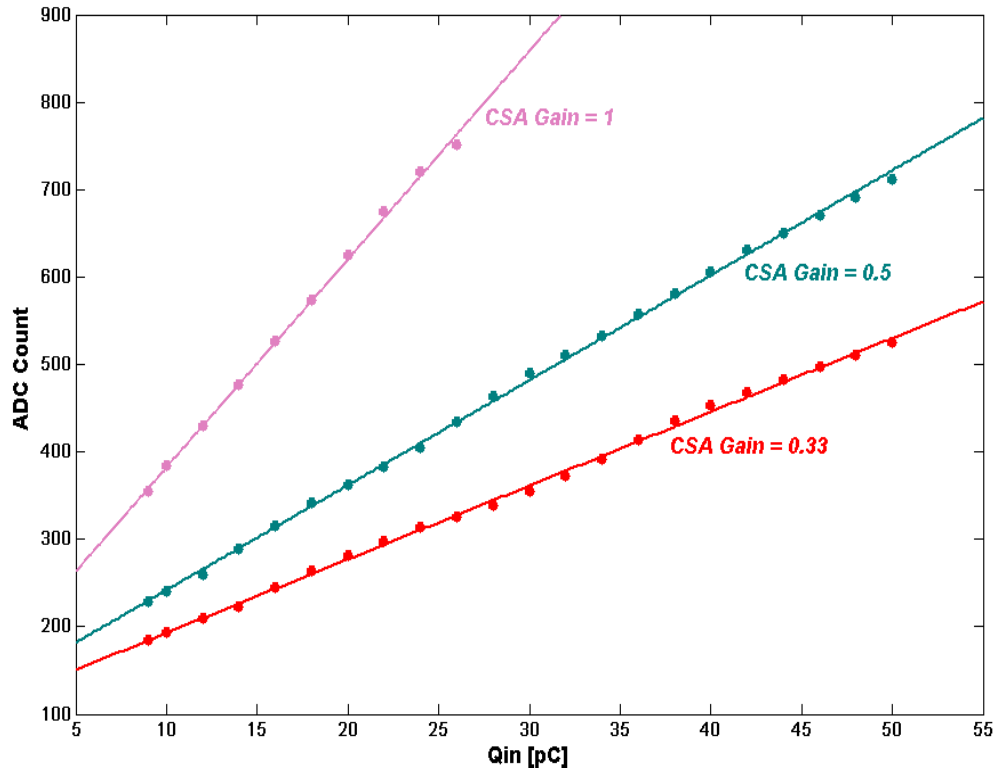
- ☐ External “coincidence” signal:
*In internal read-out mode, the
acquisition is conditioned by this signal*

Experimental results: pedestals



- ❑ Acquisition mode: internal read-out , external trigger, serial
- ❑ The “test_pd” signal of the PD’s is controlled externally, to avoid the discharge of the Cs capacitance during the “hold=1” phase
- ❑ An ADC count corresponds to about 3.9 mV
- ❑ Pedestals quite uniform
- ❑ Some channels exhibit more noise than the average, i.e. about 1.7mV rms, corresponding to 50fC rms

Experimental results: injection capacitance, gain



**Charge to voltage gain
of the analog channel**

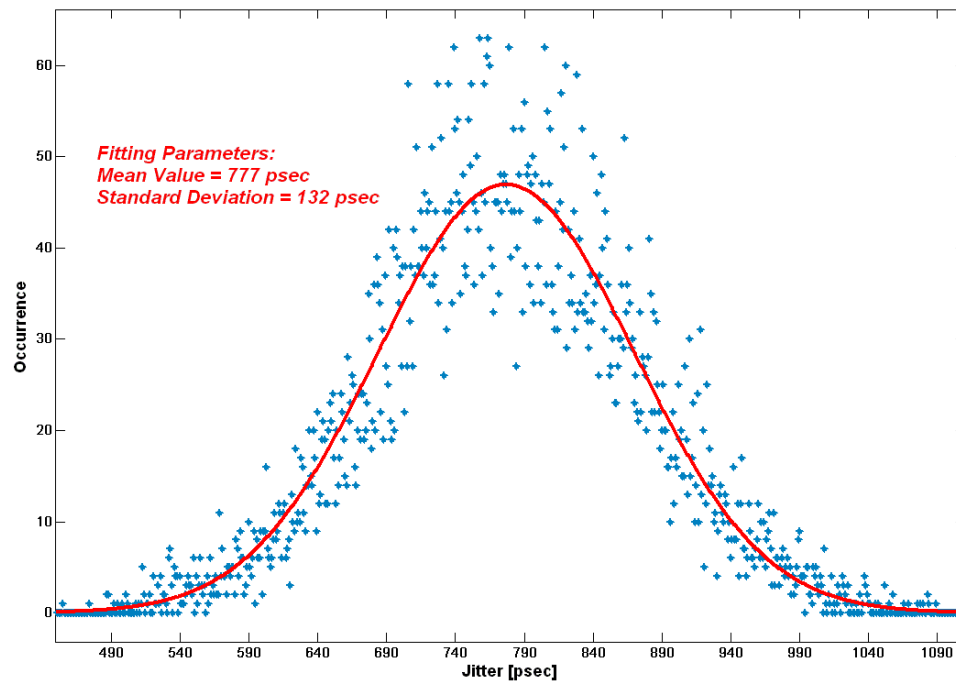
$$\frac{\Delta V_{OUT}}{Q_{in}} = \frac{1}{NC_F}$$

C_F	1pF	2pF	3pF
EXPECTED GAIN	100	50	33
MEASURED GAIN	94	47	33

**Expected and measured values of the gain
 $\Delta V_{OUT}/Q_{in}$ [mV/pC]**

- ❑ Overall charge to voltage gain very close to the expected one (max. deviation $\cong 6\%$)
- ❑ Max dynamic range $\cong 70\text{pC}$ @ $C_F=3\text{pF}$ (1% linearity error)

Experimental results: injection capacitance, timing



- *Measured standard deviation*

$$\sigma_{\text{meas}} \cong 130 \text{ ps}$$

- *Intrinsic error of the measurement setup*

$$\sigma_{\text{setup}} \cong 60 \text{ ps}$$

- *Resulting intrinsic timing accuracy of the fast-OR signal*

$$\sigma_{\text{int}} \cong 115 \text{ ps}$$

Timing accuracy of the fast-OR response vs the input pulse

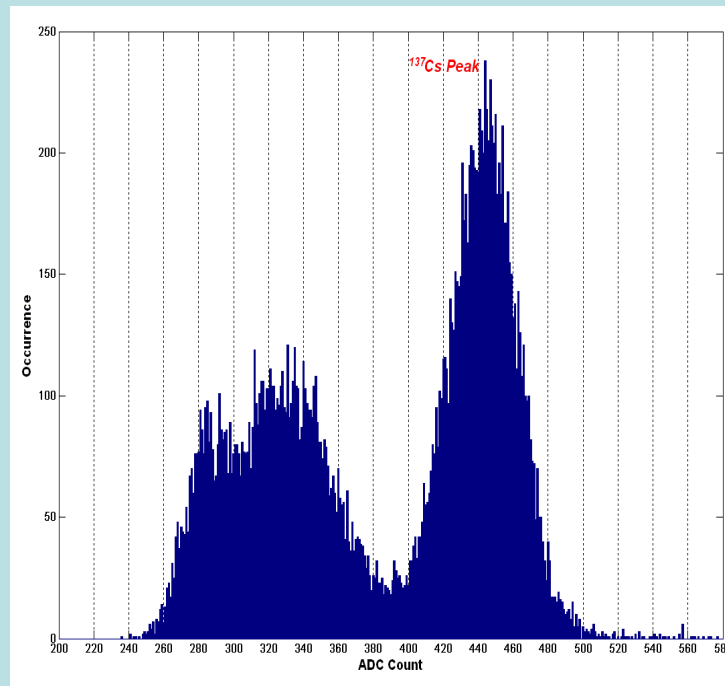
Experimental results: coupling to SiPM+scintillator (I)

- SiPMs from Hamamatsu a) 3600 micro-cells, $3 \times 3 \text{ mm}^2$, (gain = 7.5×10^5 @ $V_{\text{BIAS}} = 71.3 \text{ V}$)
b) 782 micro-cells, $3.22 \times 1.19 \text{ mm}^2$, (gain = 1.3×10^5 @ $V_{\text{BIAS}} = 71.2 \text{ V}$)
- SiPMs coupled to a small LYSO scintillator $3 \times 3 \times 10 \text{ mm}^3$
- The SiPM+LYSO detector has been coupled to a channel of the ASIC and exposed to different radiation sources:

^{176}Lu (203keV and 307keV), ^{22}Na (511keV), ^{137}Cs (662keV), ^{57}Co (122keV)



Hamamatsu SiPM coupled to the LYSO crystal

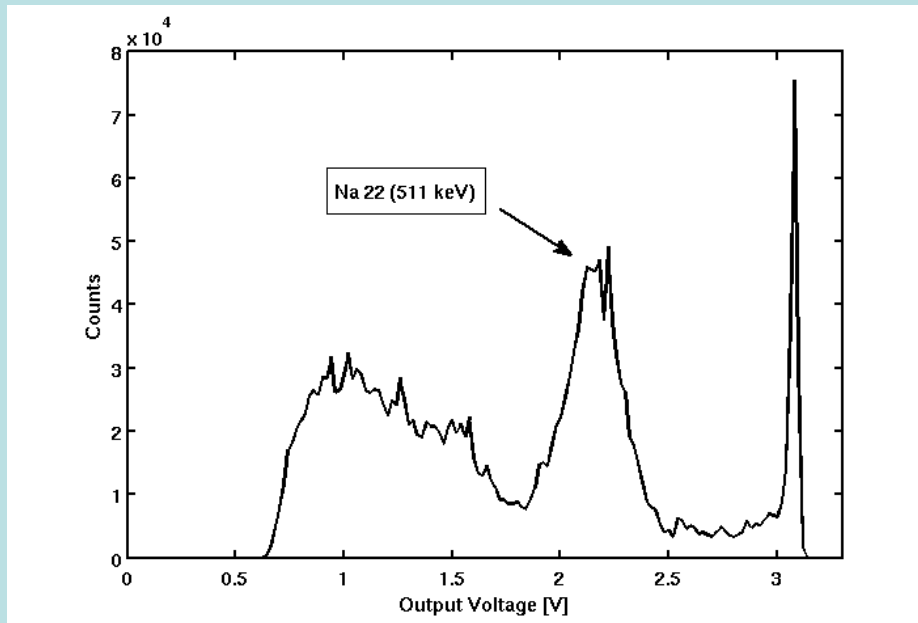


Example of ^{137}Cs spectrum ($\cong 12\%$ FWHM)

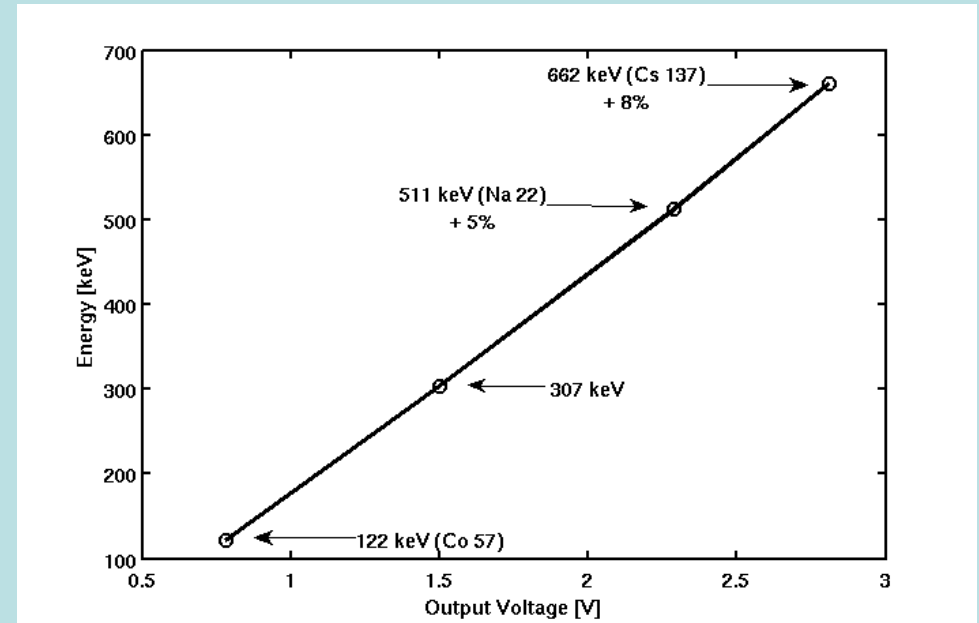
- $3 \times 3 \text{ mm}^2$ SiPM
- $V_{\text{BIAS}} = 70.2 \text{ V}$
- Gain = 33mV/pC

Experimental results: coupling to SiPM+scintillator (II)

- 782 micro-cells Hamamatsu SiPM, $V_{BIAS} = 70V$, gain = 0.33mV/pC



Spectrum of ^{22}Na (about 22% FWHM)

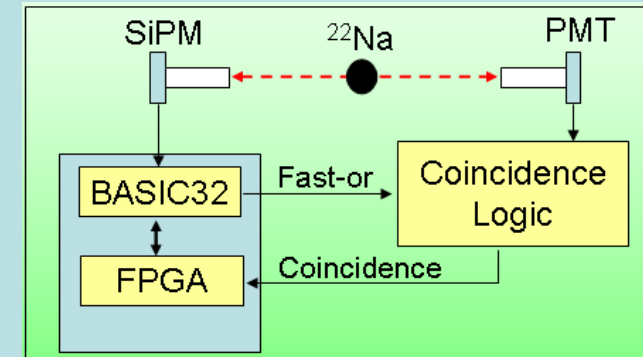
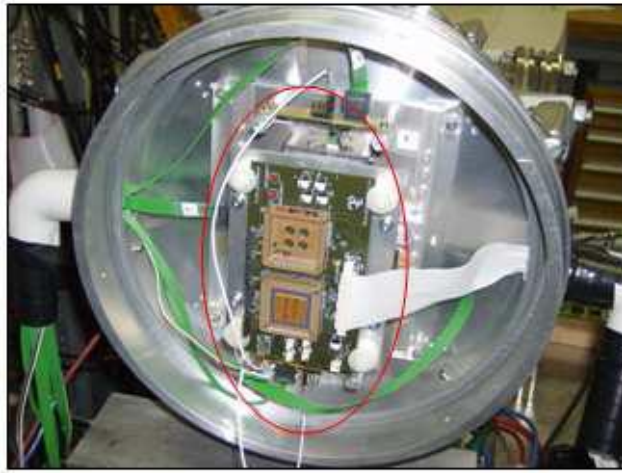


Energy vs average output voltage for the different sources

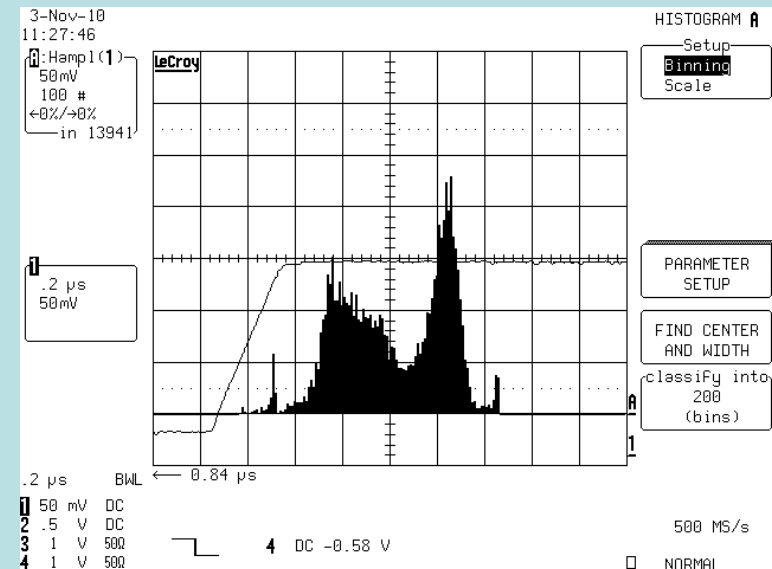
- Corrections applied to compensate for SiPM saturation (large no. of fired micro-cells)

Measurements of SiPM in coincidence with a PMT (I)

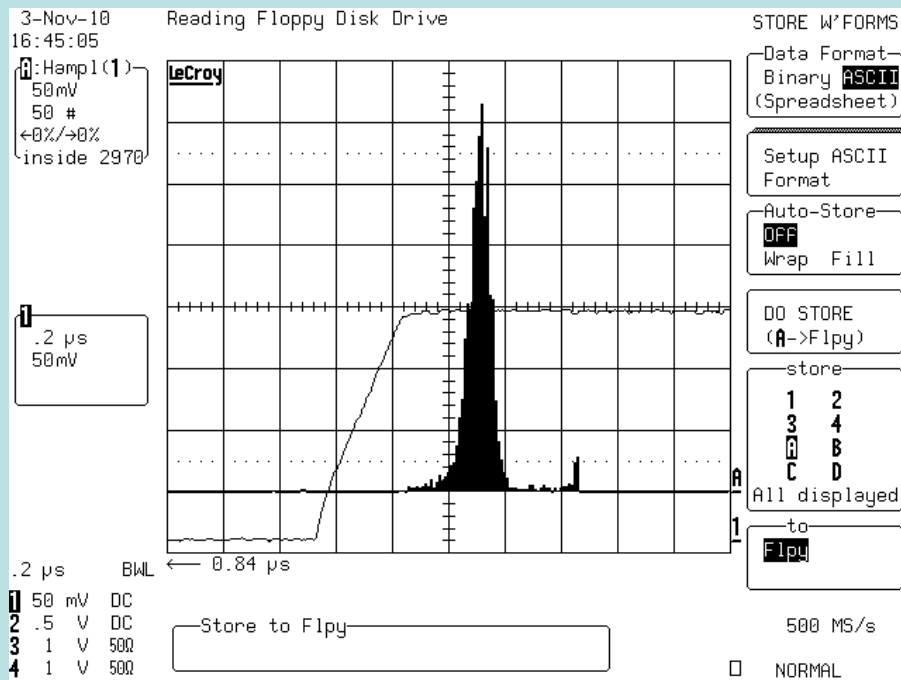
Measurement setup at CERN (courtesy of E. Chesi, A. Rudge and J. Seguinot)



- ❑ *Measurements taken in coincidence with a PMT*
- ❑ *Very low event rate ($\cong 1.9$ Hz)*
- ❑ *Signals acquired with an oscilloscope*
- ❑ *Spectrum of ^{22}Na spectrum very similar to the one shown in the previous slide (low threshold)*

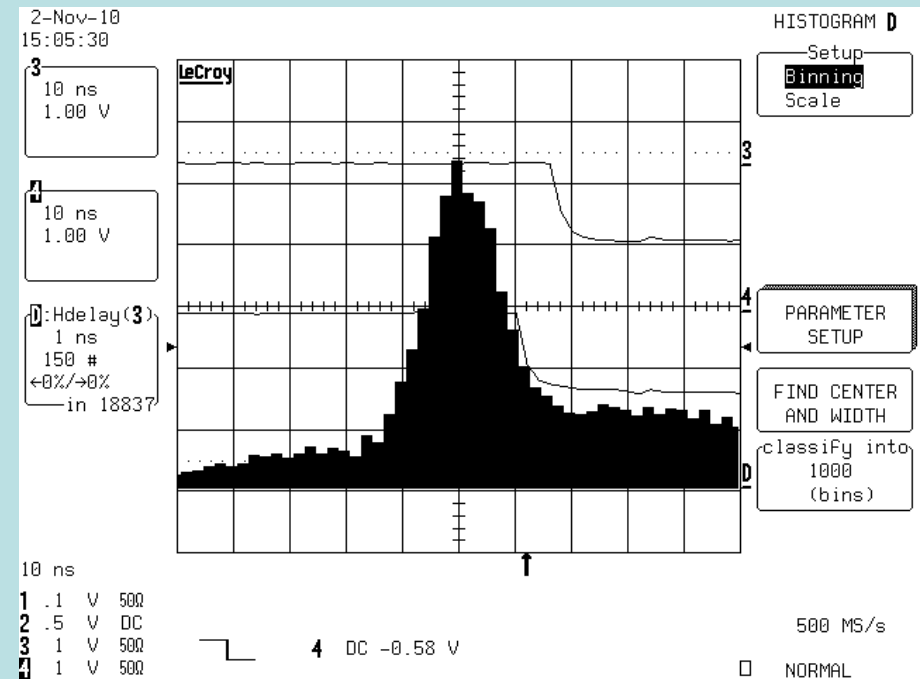


Measurements of SiPM in coincidence with a PMT (II)



Energy spectrum of ^{22}Na

- Threshold increased to get rid of the Comptons:
energy resolution $\cong 11\%$ FWHM



*Timing accuracy of the fast-OR signal
vs the trigger provided by the PMT*

- Low threshold level:
timing accuracy $\cong 1.2$ ns FWHM

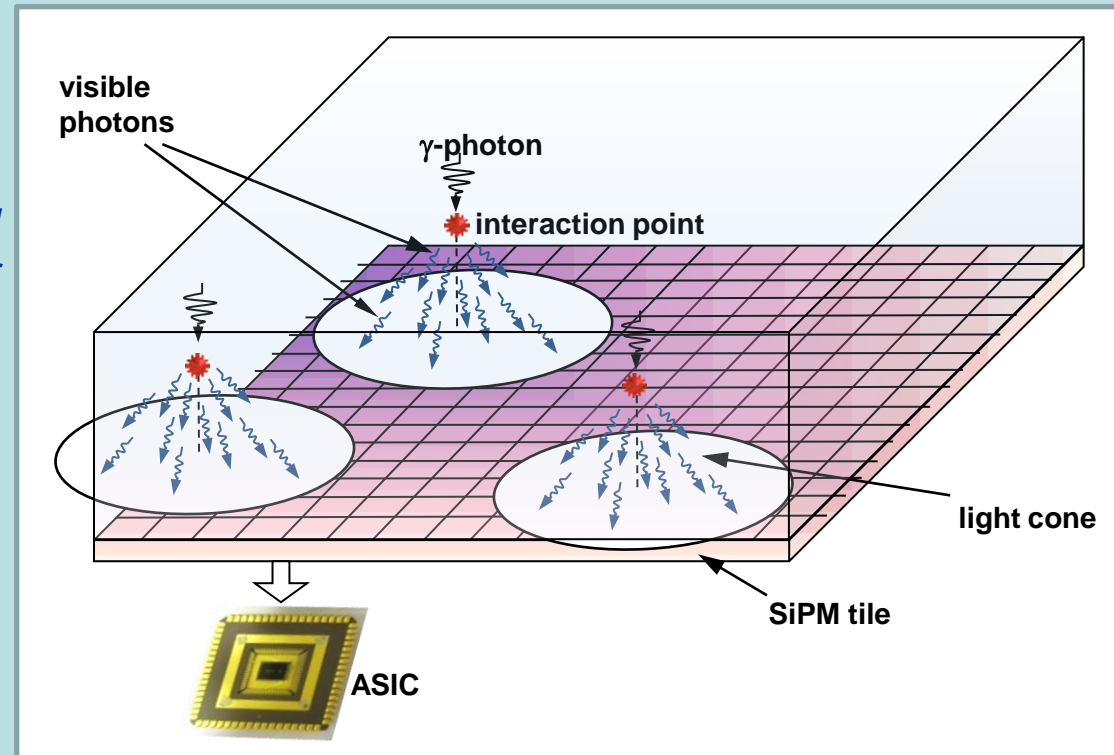
A different architecture: motivations

Application: continuous scintillator slab

The Depth Of Interaction information can be related to the asymmetry of the cluster of SiPM found over threshold on the two sides of the scintillator

SiPMs at the border of the cluster receive a small total number of photons, distributed in time according to the time constant of the scintillator

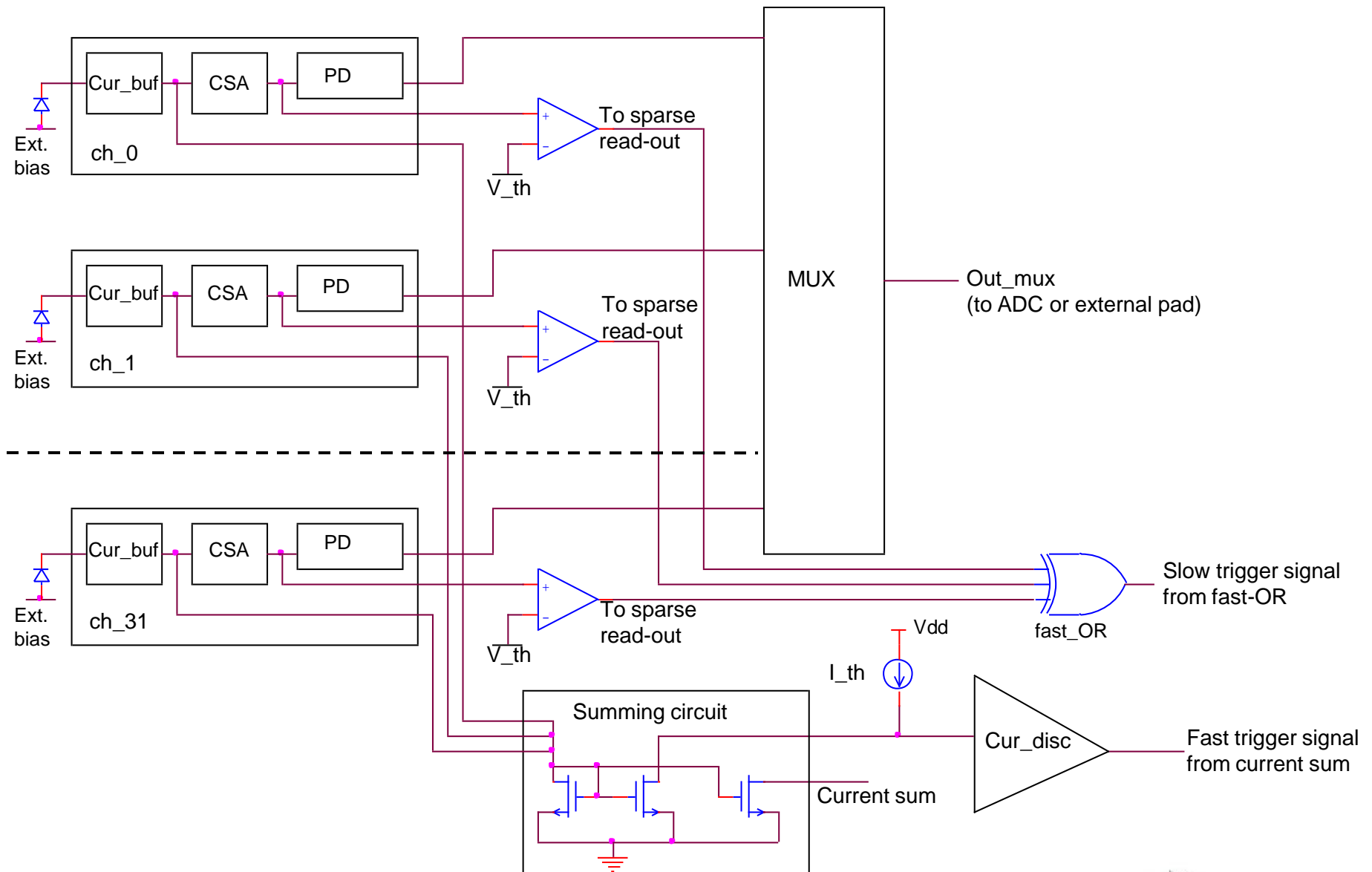
The current signal can be under the threshold set on the current level, thus they would be ignored in a sparse read-out acquisition



Proposed solution

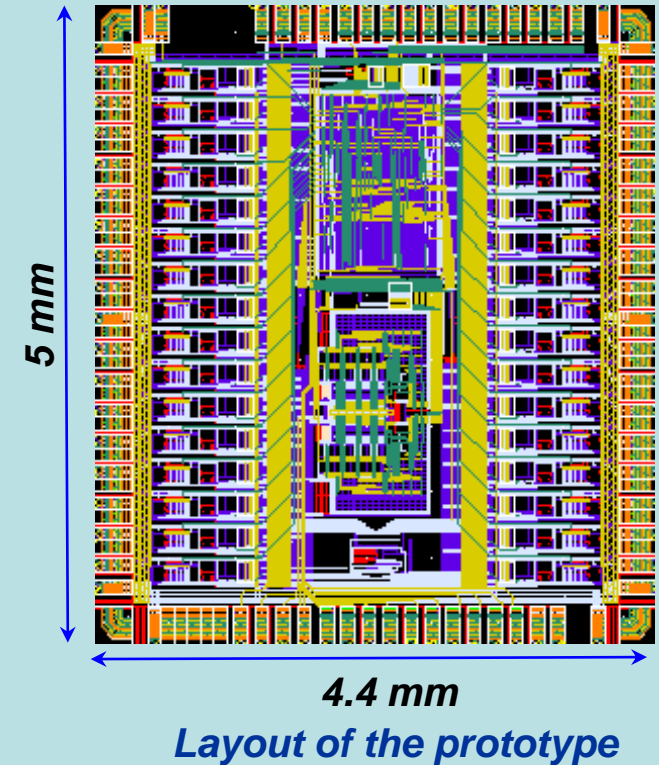
- 1) Sum of the current pulses from all the channels (exploiting the “fast” signal path of the FE)
- 2) Current discriminator which fires when the **sum** of the currents overcomes the threshold
- 3) Voltage discriminator at the “**charge**” output of each channel (“slow” signal path), instead of the current discriminator in the “fast” signal path, to make effective the sparse read-out operation

New proposed architecture



Last version of the ASIC: BASIC32_ADC

- ❑ *Internal 8-bit subranging ADC*
- ❑ *Extended dynamic range (more than 100pC)*
- ❑ *Improved configuration flexibility (524 bits) (channels configurable independently)*
- ❑ *Analog current sum output*
- ❑ *Analog multiplicity output*
- ❑ *The internal read-out procedure can be started by the “slow” (fast-OR of the voltage comparators) or “fast” (current discriminator) trigger*
- ❑ *Currently in test phase*



SiPM gain: temperature dependence

$$G=Q/e=[C_{\text{pixel}} (V_{\text{BIAS}}-V_{\text{BR}})]/e$$

SiPM gain

C_{pixel} = total capacitance of the single micro-cell

V_{BIAS} = detector bias voltage

V_{BR} = breakdown voltage

❑ Breakdown voltage temperature dependence:

$$V_{\text{BR}}(T)=V_{\text{BR}0}[1+\beta(T-T_0)]$$

β order of magnitude: $10^{-3} / ^\circ\text{C}$

❑ Gain temperature dependence:

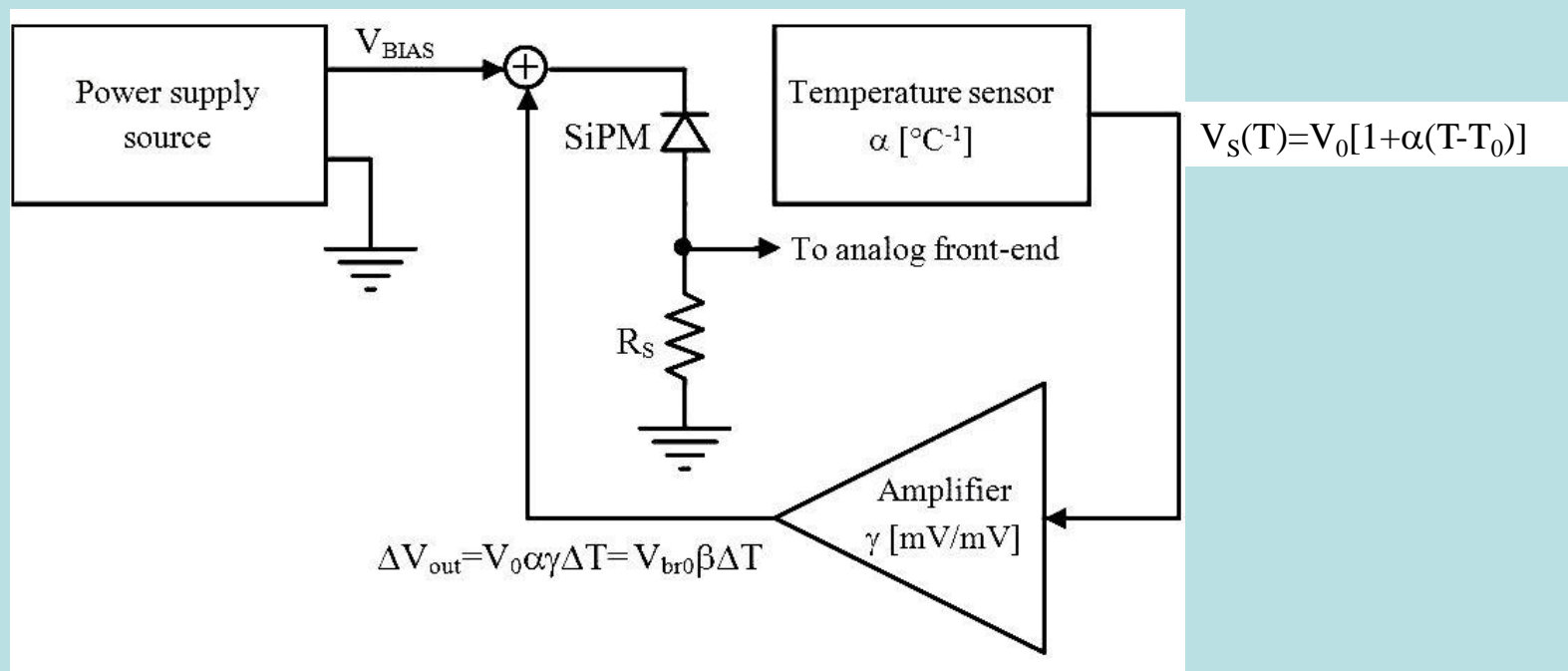
$$\frac{dG}{dT} = -\frac{C_{\text{pixel}}}{e} V_{\text{BR}0} \beta$$

better than APD, but still a problem to be addressed

Solutions proposed in the literature

Based on open loop techniques:

- a. Measurement of parameter β
- b. Measurement of the temperature (using a sensor)
- c. SiPM bias voltage adjustment $\Delta V_{\text{BIAS}} = \Delta V_{\text{BR}}(T)$

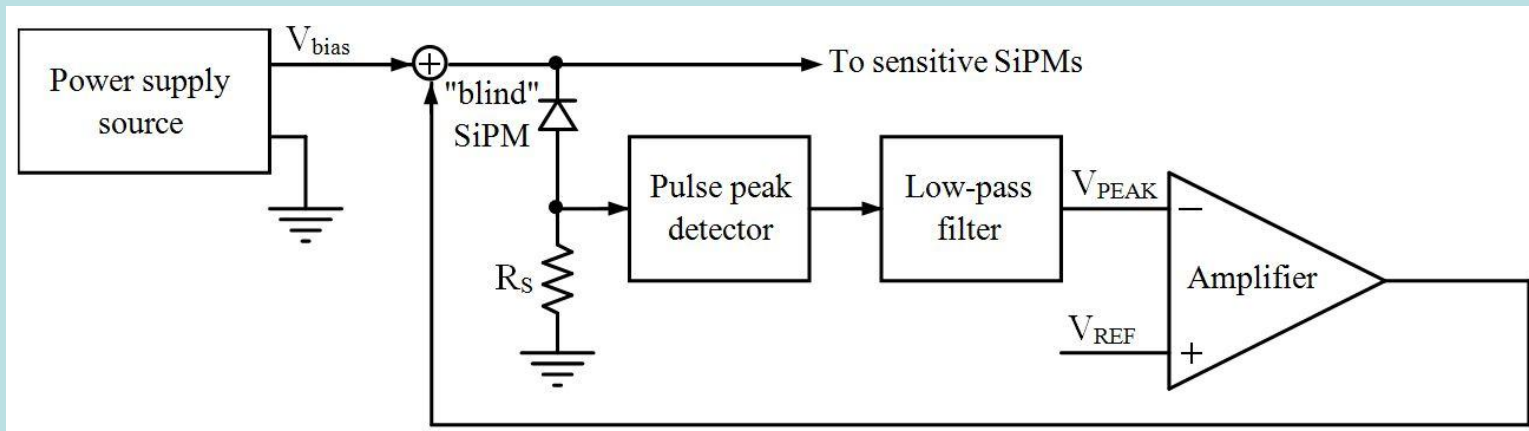


Parameters β , α and γ must be known and/or controlled with good accuracy

New proposed solution

Closed loop technique:

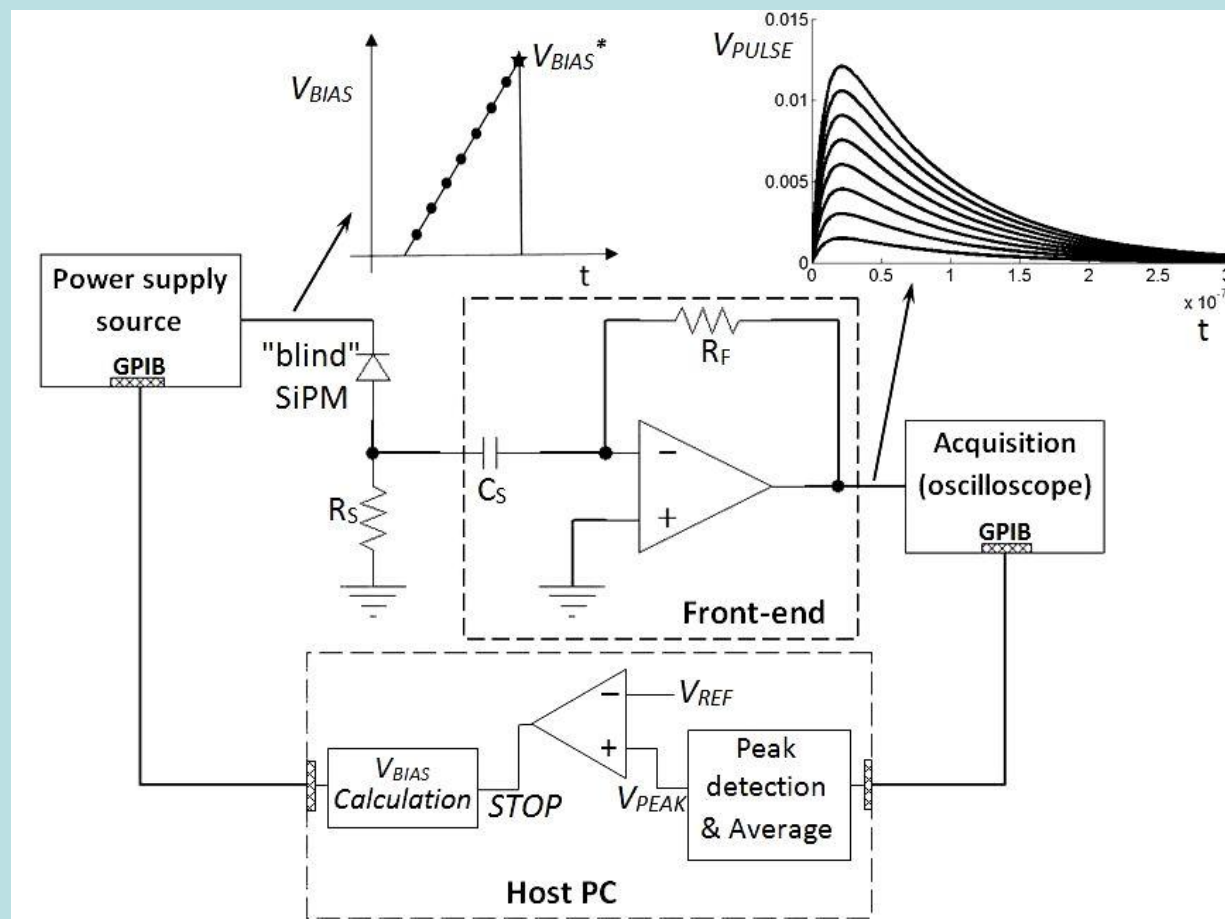
- A SiPM not exposed to incident photons ("blind" SiPM) is used as a temperature sensor
- Measurement of the average dark pulse amplitude V_{PEAK} of the blind SiPM (proportional to the gain)
- Blind SiPM bias voltage automatically adjusted by a feedback loop to make V_{PEAK} (thus the gain) constant and equal to a reference value V_{REF}



Main requirement: same β for the blind SiPM and the active detectors

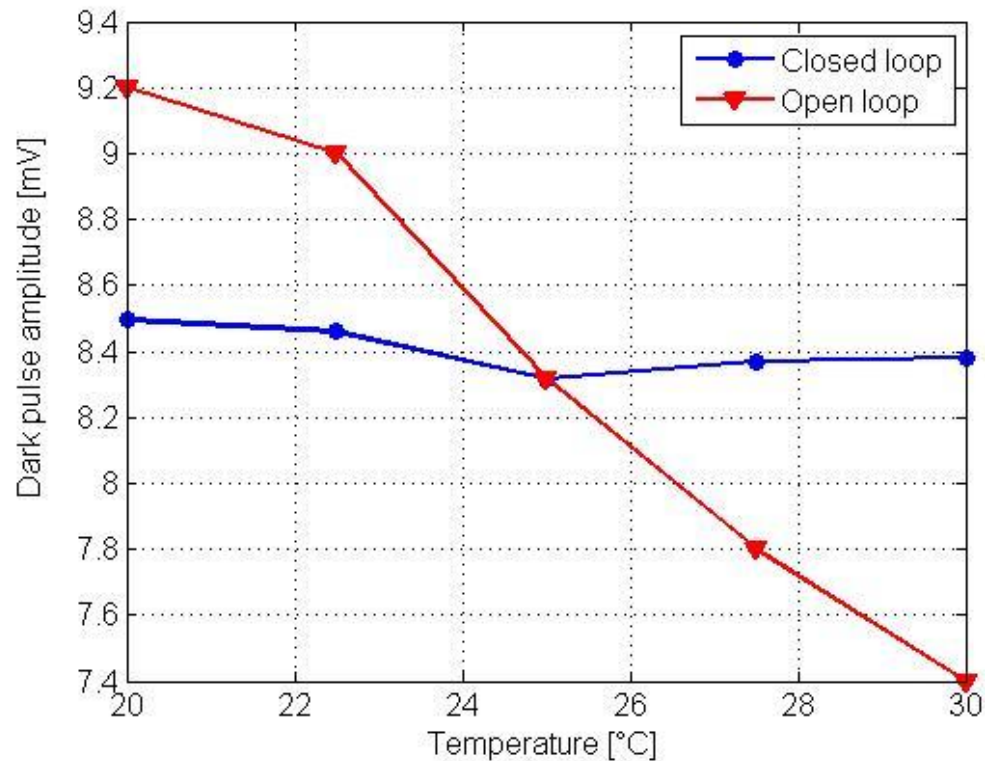
Experimental proof of principle

- Single measurement cycle: V_{BIAS} increased linearly on the blind SiPM until the desired V_{PEAK} (i.e. the required gain) is reached ($V_{BIAS} = V_{BIAS}^*$)
- Measurement cycles continuously applied : V_{BIAS}^* tracks the temperature variations and is applied to the active SiPMs



First results

- ❑ Two SiPMs from FBK-irst, 400 micro-cells, $50 \times 50 \mu\text{m}^2$ used as blind and sensitive detectors
- ❑ Temperature controlled by means of a small Peltier cell



- ❑ Open loop variation of the gain $\cong 20\%$
- ❑ Closed loop variation of the gain $\cong 2\%$

Work in progress

- ❑ Application of BASIC in a PET prototype: small animal PET (Pisa)
- ❑ Characterization of the last version of BASIC with modified architecture
- ❑ Effective circuit implementation of the temperature compensation technique
- ❑ Statistical modelling of the current pulse waveform produced by the system
scintillator + SiPM + FE electronics for timing accuracy evaluation
- ❑ Design of a new SiGe ASIC with enhanced timing capabilities